

NUMERICAL MODELLING OF FLOW AND HEAT TRANSFER FOR THE COMPRESSION RTM PROCESS WITH A FAST-CURE EPOXY

A. Keller¹, C. Dransfeld¹ and K. Masania^{2*}

1. Institute of Polymer Engineering, FHNW University of Applied Sciences and Arts Northwestern Switzerland, Klosterzelgstrasse 2, 5210 Windisch, Switzerland.

Web Page: <http://www.fhnw.ch/ikt>

2. Complex Materials Group, Department of Materials, ETH Zürich, 8093 Zurich, Switzerland

Email: kunal.masania@mat.ethz.ch, Web Page: <http://www.complex.mat.ethz.ch/>

Keywords: Heat transfer, CRTM, fast-cure, exotherm

Abstract

Fast-cure resins combined with high pressure liquid composite moulding processes (LCM) such as compression resin transfer moulding (CRTM) may be used to produce composite parts with cycle times of only a few minutes. Processing of such fast-cure resins adds difficulties to manufacturing due to the high exothermic reaction during cure, where gelation may occur before fibre impregnation. Combined modelling of rheo-kinetics, flow and heat transfer can help optimising the process parameters and ensure complete impregnation without sacrificing cycle time. The numerical model developed in this study was used to model the CRTM process for a 4 mm plate with a mould temperature of 100 °C. It was shown that cure times of a few minutes are possible with the studied epoxy but large variations of the degree of cure at different locations over the thickness can occur.

1. INTRODUCTION

Liquid composite moulding processes (LCM) are widely used for production of composite parts and may be seen advantageous for high volume production of parts with short cycle times and lower cost when compared to standard manufacturing processes such as prepreg / autoclave. However, the interplay of process parameters such as cure temperature or injection strategy must be carefully understood in order to minimise cycle time and costs without sacrificing part quality.

When using fast-cure resins with cure times of only a few minutes, manufacturers move towards high pressure LCM processes such as high pressure resin transfer moulding (HP-RTM) or compression RTM (CRTM) [1]. The through thickness flow in CRTM reduces the impregnation length, and hence the impregnation time by orders of magnitude, allowing the use of fast-cure resins [2]. Baskaran et al. [1] showed in their study that the manufacturing cost of an automotive roof can be reduced by using CRTM compared to HP-RTM. A schematic of the CRTM process is shown in Figure 1 and described in chapter 3. Several numerical models for the CRTM process have been proposed [3-6].

However, the use of fast-cure resins results in new challenges regarding handling of the material and injection. One of the major difficulties with fast-cure resins is their exothermic reaction during cure, resulting in a significant temperature overshoot compared to the mould [7], which may cause resin gelation before impregnation and/or gradients in temperature and degree of cure inside the part, internal stresses or even material decomposition. Modelling of the cure reaction during injection, impregnation and cure stages may be used to optimise the cycle time without sacrificing part quality.

Cure optimisation models for thick composite parts [8] aim to reduce the temperature gradient during cure, which is also necessary when using fast-curing, highly reactive resin systems in order to optimise cycle time and minimise cure induced stresses [9]. The use of fast-cure resins further requires modelling of the injection process, as resin gelation may occur before the preform is fully saturated.

The aim of this study is to investigate the exothermic reaction, the resulting temperature gradient and degree of cure variation over the thickness of a composite plate during cure (Stage 2 of the CRTM

process) via numerical models. Effects of resin flow, heat transfer, rheo-kinetics, changing part thickness and preform permeability were taken into account.

2. MATERIALS

The materials used for the experimental validation are the XB3585/XB3458 epoxy from Huntsman and a carbon unidirectional weave fabric with 3K tows and an aerial weight of 140 g/m². Their properties are likewise considered in the numerical models.

3. COMPRESSION RESIN TRANSFER MOULDING

The CRTM Process (displayed in Figure 1) typically starts by adding the reinforcement into the preheated tool and casting resin over the preform (as was done in this study) or injecting resin through a gap. The resulting heat transfer between the preheated preform and the resin results in an increasing resin temperature, and hence decreasing viscosity. Impregnation due to gravity and capillary forces may be possible in this stage, depending on the preform permeability and resin viscosity (Figure 1: Stage 1b). These steps are summarised as stage 1.

With standard, slow curing epoxies the heat transfer in this stage, assuming an isothermal mould temperature, is of less importance. Impregnation may be started after temperature equilibration.

However, with fast-cure resin systems, the increasing temperature can start the curing reaction, leading to a high exothermic temperature overshoot. This can not only lead to resin gelation before the preform is fully impregnated, but also lead to resin decomposition (Figure 1: “Resin gelation and possible decomposition”). Hence, the start of impregnation due to the closing velocity of the upper mould part needs to be optimised to avoid this phenomena.

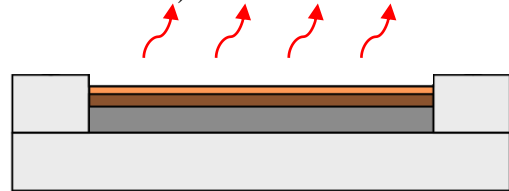
When mould closing and resulting impregnation and compaction starts in time (Figure 1: Stage 2), the part can be cured and ejected. A high fibre volume content does reduce the exothermic mass, and hence helps to reduce the exothermic temperature overshoot. Nevertheless, care has to be taken during cure to avoid high temperature variation over the thickness in order to minimise internal stress generation during cure.

Stage 1

Stage 1a) Resin is poured on top of a preheated preform and mould

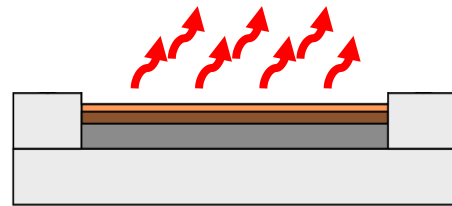


Stage 1b) Heat transfer between preform and resin → resin viscosity decreases and impregnation starts (gravity and capillary driven, no external force)



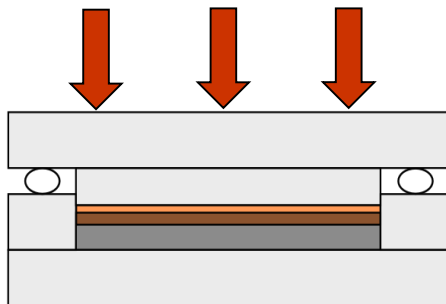
$t_{\text{start_of_impregnation}} > t_{\text{gelation}} \rightarrow$ **Resin gelation and possible decomposition**

Stage 1 c) The time to start impregnation due to the closing motion of the upper mould part is too long.
 → Stop of impregnation due to resin gelation and possible decomposition

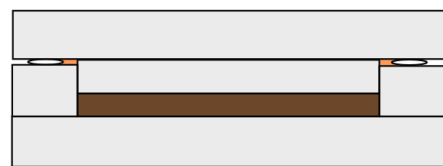


$t_{\text{start_of_impregnation}} < t_{\text{gelation}} \rightarrow$ **Stage 2**

Start of impregnation and compaction in time



Stage 2a) Impregnation and compaction



Stage 2b) Cure and ejection

Figure 1. Schematic of the compression resin transfer moulding (CRTM) process.

4. GOVERNING EQUATIONS AND MATERIAL PARAMETERS

4.1 Flow

Darcy's law is typically used to model the viscous flow through a porous media. Combined with mass conservation and a source term to account for the preform compaction; Darcy's law results in.

$$\nabla \cdot \left(-\frac{K}{\eta} \nabla p \right) = -\frac{1}{V_f} \frac{\partial V_f}{\partial t} \quad (1)$$

Where v is the flow velocity, K is the permeability V_f The fibre volume content and η the viscosity.

A pressure gradient can be observed during impregnation in through thickness direction. Terzaghis's law [10] was used to model the pressure gradient of the resin and the preform during combined impregnation and compaction.

$$p_{ap} = \sigma_{pref} + p \quad (2)$$

Where p_{ap} is the applied pressure from the top mould, σ_{pref} the preform stress and p the fluid pressure.

A level set method was used to track the flow front in the following form, as implemented in Comsol Multiphysics 5.0 [11]:

$$\frac{\partial \phi}{\partial t} + u \cdot \nabla \phi = \gamma \nabla \cdot \left(\varepsilon_{ls} \nabla \phi - \phi(1 - \phi) \frac{\nabla \phi}{|\nabla \phi|} \right) \quad (3)$$

Where the reinitialisation parameter, γ is used to compute the steady state solution after each time step to avoid numerical smearing and ε_{ls} controls the interface thickness.

A smoothing function was implemented to reduce numerical noise.

$$\phi_{smooth} = \frac{1}{1 + \exp(\delta(-\phi + 0.5))} \quad (4)$$

Where the parameter δ is used to define the width of the transition region.

4.2 Heat transfer

The resin and composite temperature were calculated with the heat transfer equation and a source term, representing the internal heat generation of the epoxy during cure,

$$\rho_c C_p \frac{\partial T}{\partial t} + \rho_r C_{pr} v \cdot \nabla T + \nabla \cdot (-k \nabla T) = \rho_r H_{tot} \frac{d\alpha}{dt} (1 - V_f) \quad (5)$$

where T is the temperature, ρ_r and ρ_c are the densities of the resin and the composite respectively, C_p the heat capacity, v the volume averaged Darcy velocity, k the thermal conductivity tensor, H_{tot} the total heat of reaction, $d\alpha/dt$ the reaction rate and V_f the fibre volume fraction.

Table 1. Material parameters for the heat transfer equation.

	Epoxy	Preform
Heat conductivity, k (W/(m K))	0.2	1.7
Specific heat capacity, C_p (J/(kg K))	1336+9.3T (°C)	577+6.85T (°C)- 0.018T ² (°C) [12]
Density, ρ (kg/m ³)	1150	1700

4.3 Rheo-kinetics

The reaction rate in eq. (5) was previously modelled [7], based on the approach of Ruiz et al. [13].

$$\frac{d\alpha}{dt} = k_1 e^{\left(-E_1 \left(\frac{T_{ref}-T}{T}\right)\right)} \sum_{i=0}^m G_i \alpha^i (\alpha_{max}(T) - \alpha)^n \quad (6)$$

$$\text{With } G(\alpha) = \frac{G_1 \alpha^4 + G_2 \alpha^3 + G_3 \alpha^2 + G_4 \alpha + G_5}{G_6 \alpha^2 + G_7 \alpha}$$

$$\alpha_{max} = \frac{T_c - T_{g0}}{(T_c - T_{g0})(1 - \lambda) + (T_{g\infty} - T_{g0})\lambda}$$

$$\text{and } n = n_s \cdot T_c + n_i$$

The modelling parameters are presented in Table 2.

Table 2. Parameters of the kinetic model

Parameter	Value	Parameter	Value
Polynomial parameter, G ₁	-1351	Reaction exponent factor slope, n _s	0.018
Polynomial parameter, G ₂	-2678	Reaction exponent factor intercept, n _i	-5.2367
Polynomial parameter, G ₃	10194	Frequency factor, k ₁ (1/s)	0.00309
Polynomial parameter, G ₄	4338	Activation energy, E ₁	22.28
Polynomial parameter, G ₅	-5.208	Reference temperature, T _{ref} (K)	350
Polynomial parameter, G ₆	587	T _g of the uncured resin, T _{g0} (K)	246.15
Polynomial parameter, G ₇	4570	T _g of the cured resin, T _{g∞} (K)	394.4
		Parameter for αmax model, μ	0.32

A viscosity model was implemented in the numerical models based on the approach of Kiuna et al. [14]

$$\eta(t, T) = \exp \left(\frac{\sum_i^n A_2 \exp \left(\frac{E_2}{RT} \right) t_i (A_4 T + E_4)}{E_3 \frac{1}{A_3 \exp \left(\sum_i^n A_2 \exp \left(\frac{E_2}{RT} \right) \frac{t_i (A_4 T + E_4)}{E_3} \right)}} \right) A_1 \exp \left(\frac{E_1}{RT} \right) \quad (7)$$

where t is the time, T the temperature, R the universal gas constant and A and E are fitting parameters summarized in Table 3.

Table 3. Parameters of the rheological model

Parameter	A ₁	E ₁	A ₂	E ₂	A ₃	E ₃	A ₄	E ₄
Value	1.32 x 10 ⁻⁹	52931	7518	38710	2.7	2.2	0.003	-0.409

4.4 Moving mesh

A moving mesh based on the arbitrary Lagrangian-Eulerian (ALE) method was used to account for the change of thickness of the resin film on top of the preform and during compaction of the preform.

4.5 Experimental measurement preform compaction

The compaction behaviour of the preform was measured in a Walter & Bai, Switzerland testing machine between two parallel plates with a diameter of 136 mm and a constant velocity of 0.5 mm/min. Machine compliance was measured and subtracted from the machine measured displacement. Measurements were conducted for both the dry and silicone oil impregnated wet preform, with a viscosity of 0.1 Pas to match the initial viscosity of the mixed resin at 100 °C. Up to 30 layers were used for these measurements to eliminate local effects of nesting and tow movement.

A power law model was used to fit the experimentally obtained data.

$$\sigma(V_f) = A \cdot V_f^B \quad (8)$$

Where σ is the preform stress, V_f is the fibre volume fraction and A and B are fitting parameters.

Table 4. Parameters of the preform compaction fitting

	A	B
Dry	2.23 x 10 ⁻⁹	20.3
Wet	6.25 x 10 ⁻⁷	11.3

4.6 Experimental measurement of the preform permeability

Preform samples with a diameter of 79 mm were cut on a Zünd G3 M-2500 cutter and carefully placed in a jig to measure the through thickness permeability. Measurements were performed for V_f values of 0.39 (zero compaction), 0.45, 0.55 and 0.65.

The measured permeability with a V_f value of 0.39 was analysed with an injection pressure of 0.05 bar. For higher V_f values, linear regression was used to calculate the permeability for different injection pressures that were all lower than the preform compaction pressure.

A good fit within the measured range was obtained using a second order polynomial fit.

$$K_z = 1.92 \times 10^{-11} V_f^2 - 2.72 \times 10^{-11} V_f + 9.66 \times 10^{-12} \quad (9)$$

5. NUMERICAL MODEL SET UP

The models were solved in Comsol Multiphysics 5.0 using the “MULTifrontal Massively Parallel sparse direct Solver” (MUMPS). A direct solver was preferred to ensure convergence and good results were obtained with MUMPS solver, which is set as standard solver for the studied physics. The fully coupled nonlinear solver uses the damped Newton method to obtain convergence. With this method a damping factor is varied, until the solution converges, based on the initial value.

A triangular free mesh was used and the element size was set to 0.68 mm for the model with a length of 30 mm after a convergence analysis of different mesh sizes.

A pressure curve as used as a boundary condition (BC) on the top mould, resulting from the pressure of the constant closing velocity of 0.5 mm/s in the beginning the preform stress in the later stage of the process. A zero pressure boundary condition was applied on the bottom. A constant temperature of 100 °C was applied on the top and bottom boundary. In reality the mould temperature may slightly increase its temperature after the exothermic reaction. The peak temperature itself is not significantly influenced by this boundary condition, as the exothermic reaction progresses rather quickly. A temperature increase of only 2-3 °C of the steel tool was measured experimentally. Periodic BC were applied on the left and right side to account for the effects of neighbouring fabric, whilst computing only a small part of it.

The presented model aims to calculate the temperature and degree of cure progression during cure in stage 2 of the CRTM process.

6 RESULTS OF STAGE 2

6.1 Temperature

The start of stage 2 was taken 45 s after the resin was poured over the preform. This time was experimentally determined. Although heat transfer started at this point, time and temperature were not sufficient to start the cure reaction.

The exothermic reaction lead to a maximum temperature of 115 °C in the middle of the 4 mm plate with a global V_f of 0.6. A significant increase of the reaction rate with increasing temperature can be observed, as indicated by the DSC measurements shown in Figure 2 (a). Hence, a variation of 15 °C results in a significant degree of cure variation over the thickness during cure, as discussed in the following section.

6.2 Rheo kinetics

A strong variation of the degree of cure was calculated and is shown in Figure 2 (b), with a maximum variation of 0.12 after 90 s. A gelation time of 135 s for the whole plate has been calculated, although in locations with a higher temperature overshoot, i.e. in the middle of the thickness, gelation occurred faster. The degree of cure progression is shown in Figure 2 (b) and it can be seen that the degree of cure varies between 0.69 and 0.75 over the thickness after 135 s. A fairly uniform degree of cure of 0.9 was calculated after 5 min and a maximum degree of cure of 0.92 after 7 min. This agrees well with experimentally determined degree of cure results of 0.88 – 0.93 from experimentally manufactured plates, measured with differential scanning calorimetry (DSC) and a heating rate of 10 K/min.

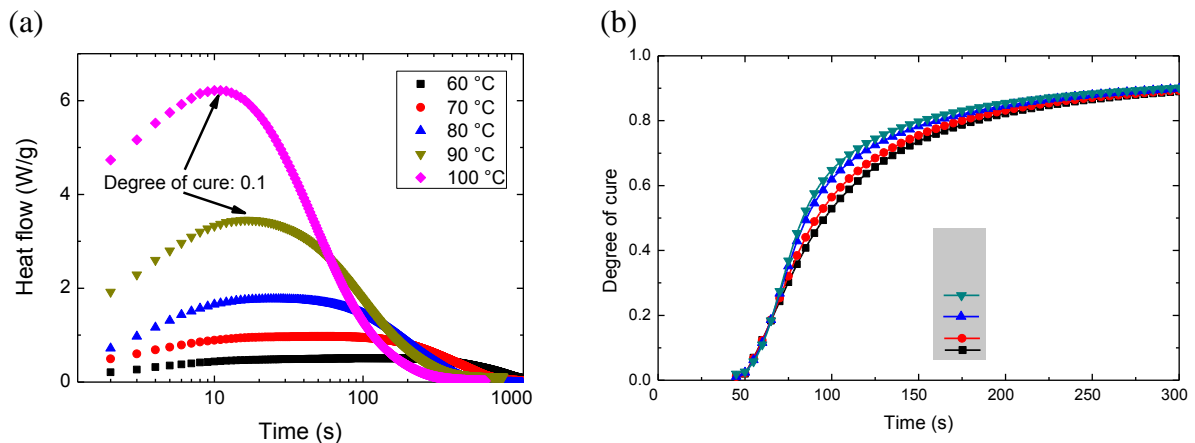


Figure 2. (a) Measured heat flow using DSC under isothermal conditions [7]. (b) Degree of cure progression over the thickness (indicated as grey area) calculated with the numerical model

Impregnation

The whole impregnation process was calculated to take about 6 s. It shall be noted that dual-scale effects of the preform have not been implemented; air formation, which may reduce the total saturation time, is not considered.

6. DISCUSSION AND CONCLUSION

Processing with fast-cure epoxies increases productivity but may result in more difficulties compared to traditional epoxies with longer cure times. These are given by the strong exothermic reaction and resulting temperature overshoot that may prevent full impregnation of a part. The large resin mass in the initial stage of the CRTM process may lead to very high temperature overshoots compared to the mould temperature, as well as very quick gelation. It was calculated that impregnation in this cases takes only about 6 s with a closing velocity of 0.5 mm/s and a maximum pressure of 20 bar. The part reached gelation after 135 s and finished curing after 7 min.

Strong gradients over the thickness of temperature and degree of cure may be observed during the cure stage. For the modelled case, the final degree of cure stabilised over the thickness by the time demoulding was conducted. However, a degree of cure variation over the thickness of up to 0.12 was calculated.

Finding the optimal processing conditions seems to be individual to a processing procedure, i.e. injection strategy, part shape and thickness. In some cases it might be necessary to reduce the temperature of the mould. The presented models aim to provide better understanding about such limitations by studying the exothermic heat during the injection, impregnation and curing stages of a CRTM process using fast-cure epoxies. These materials, combined with suitable process optimisation tools as those presented here, greatly increase the reliability of high-volume production techniques with cycle times in the order of a few minutes.

Acknowledgments

The authors would like to thank Huntsman Advanced Materials, Switzerland for supplying materials.

References

1. Baskaran, M., de Mendibil, I Ortiz; Sarrionandia, M; Aurrekoetxea, J; Acosta, J; Argarate, U; Chico, D, *Manufacturing cost comparison of RTM, HP-RTM and CRTM for an automotive roof in ECCM16*. 2014: Sevilla, Spain.
2. Masania, K., B. Bachmann, and C. Dransfeld. *The compression resin transfer moulding process for efficient composite manufacture*. 2012. ICCM.

3. Pham, X.-T., Trochu, François; Gauvin, Raymond, *Simulation of compression resin transfer molding with displacement control*. Journal of reinforced plastics and composites, 1998. **17**(17): p. 1525-1556.
4. Shojaei, A., *Numerical simulation of three-dimensional flow and analysis of filling process in compression resin transfer moulding*. Composites Part A: Applied Science and Manufacturing, 2006. **37**(9): p. 1434-1450.
5. Bhat, P., Merotte, Justin; Simacek, Pavel; and S.G. Advani, *Process analysis of compression resin transfer molding*. Composites Part A: Applied science and manufacturing, 2009. **40**(4): p. 431-441.
6. Gupta, A., Kelly, PA; Ehr Gott, M; Bickerton, S, *A surrogate model based evolutionary game-theoretic approach for optimizing non-isothermal compression RTM processes*. Composites Science and Technology, 2013. **84**: p. 92-100.
7. Keller, A., Masania, K; Taylor, AC; Dransfeld, C, *Fast-curing epoxy polymers with silica nanoparticles: properties and rheo-kinetic modelling*. Journal of Materials Science, 2016. **51**(1): p. 236-251.
8. Michaud, D., A. Beris, and P. Dhurjati, *Curing behavior of thick-sectioned RTM composites*. Journal of composite materials, 1998. **32**(14): p. 1273-1296.
9. Ruiz, E. and F. Trochu, *Multi-criteria thermal optimization in liquid composite molding to reduce processing stresses and cycle time*. Composites Part A: Applied Science and Manufacturing, 2006. **37**(6): p. 913-924.
10. Terzaghi, K., R.B. Peck, and G. Mesri, *Soil mechanics in engineering practice*. 1996: John Wiley & Sons.
11. Multiphysics, C., *COMSOL Multiphysics Reference Manual*. 2013, COMSOL.
12. Villière, M., Lecoite, Damien; Sobotka, Vincent; Boyard, Nicolas; Delaunay, Didier, *Experimental determination and modeling of thermal conductivity tensor of carbon/epoxy composite*. Composites Part A: Applied Science and Manufacturing, 2013. **46**: p. 60-68.
13. Ruiz, E. and F. Trochu, *Thermomechanical properties during cure of glass-polyester RTM composites: elastic and viscoelastic modeling*. Journal of Composite Materials, 2005. **39**(10): p. 881-916.
14. Kiuna, N., Lawrence, CJ; Fontana, QPV; Lee, PD; Selerland, T; Spelt, PDM, *A model for resin viscosity during cure in the resin transfer moulding process*. Composites Part A: Applied Science and Manufacturing, 2002. **33**(11): p. 1497-1503.